NP PAVONIS : DIFFERENTIAL CORRECTIONS ANALYSIS OF THE *UBV* OBSERVATIONS

M. A. Cerruti[1,2]

Instituto de Astronomía y Física del Espacio, Argentina

RESUMEN

Se presenta el primer análisis fotoeléctrico de la binaria NP Pav basado en curvas de luz U, B y V y modelado usando el tratamiento de Wilson & Devinney. Las curvas están definidas por 3861 observaciones individuales. Las componentes y la órbita parecen, en general, ser estables. La primaria, más masiva y más luminosa, es la componente de mayor tamaño y está eclipsada en el mínimo primario y no llena su lóbulo de Roche (94%). La secundaria prácticamente llena su lóbulo de Roche (99%) y tiene una diferencia de temperatura de $\Delta = -1330^\circ$K. Los elementos absolutos se obtuvieron suponiendo que la primaria sigue la relación masa-luminosidad.

ABSTRACT

The first photoelectric analysis of the NP Pav binary system based on U, B, and V light curves and modeled using the Wilson & Devinney approach, is presented. The light curves are defined by 3861 individual observations. The components and the orbit appears to be in general stable. The primary, more massive, more luminous is the greater component, eclipsed at primary minimum and is detached from its Roche lobe (94%). The secondary nearly fills its Roche lobe (99%) and has a temperature difference of $\Delta = -1330^\circ$K. The absolute elements were obtained supposing that the primary follows the mass-luminosity relation.

Key Words: **BINARIES: CLOSE — BINARIES: ECLIPSING — STARS: INDIVIDUAL (NP PAV)**

1. INTRODUCTION

NP Pav = S 5117 = KSP 5263 = BV 1305 = GSC 9321:1055 was discovered by Hoffmeister (1949) who also published a finder chart (1957). Its nature as an eclipsing binary was established by Shaw & Sievers (1970) giving a type EA light curve. They determined $10^m.7$ at maximum light and an amplitude of $1^m.0$, they observed minima giving a period of $1^d.266821$, published another finding chart, and said that it had a deep minimum II. The binary was named by Kukarkin et al. (1972). Cerruti (2000) published the first determinations of photoelectric minima showing the existence of a shallow secondary minimum not previously detected, (thus reducing by half the period), as well as a study of

the period. That is the reason why this binary was included among other binaries to study photoelectric lights curves.

To study NP Pav, we have chosen the WD eclipsing binary computer model (Wilson & Devinney 1971; Wilson 1979; Kang & Wilson 1989; Wilson 1990) because it is the standard method of treatment. We used the 1995 version of WD kindly supplied by Prof. R. E. Wilson. The main purpose of the present note is to derive the photoelectric elements of this system using all the information available.

2. OBSERVATIONS

An observation is defined here as the mean of two readings through a filter, interpolated at a common reference time in the usual symmetrical pattern f1 f2 f3 f3 f2 f1. The data used throughout this note consist of 1287 observations in each filter U, B, and V made at Cerro Tololo Inter-American Observatory in Chile with the Lowell 61 cm telescope, a single-channel photometer,

---

[1]Visiting Astronomer, Cerro Tololo Inter-American Observatory, NOAO operated by AURA Inc. under cooperative agreement with the NSF.

[2]Member of the Carrera del Investigador Científico, CONICET, Buenos Aires, Argentina.

a refrigerated RCA31034A cathode, the standard *UBV* Johnson filters, and photon-counting techniques. Observations were made alternatively for the variable and the comparison star (chosen to be closest in distance, magnitude, and color); they were freed from sky background and converted to out-of-atmosphere magnitudes, and then the difference variable-minus-comparison star was computed. The out-of-atmosphere magnitudes were calculated taken into account the nightly total extinction coefficients derived from the comparison star. The light of the comparison star CPD $-69^o3134(9.6)$ = GSC 9308:1513 was checked against SAO 254907 = HD 198971(B9/9.5 V, 6.9) = CPD -69^o3146 = CoD $-69^o1958(7.1)$ = GSC 9321:1105 = check #1, and found to be constant within the observational accuracy throughout the observing periods. Also the check #2 = HD 196784(F6/7 IV, 8.6) = CPD $-69^o3130(8.2)$ = CoD $-69^o1943(7.9)$ = GSC 9308:1782 was used. The set of individual *UBV* observations has been deposited in the IAU Archives of Unpublished Observations of Variable Stars (Schmidt 1992) under file number E344.

3. LIGHT CURVES

The vertically-shifted *UBV* differential light curves in the instrumental system are depicted in the lower part of Fig. 2. Phases were calculated using the ephemerides given by equation (1) in Cerruti (2000), that is

$$\begin{aligned} \text{Min I} \quad = \quad & \text{HJD } 2445984^d.7095(11) \\ + \quad & 0^d.63353658(20) \text{ E}. \end{aligned} \quad (1)$$

The observations show a β Lyrae light curve. The maxima are nearly of the same height for each light curve. Primary minimum corresponds to the transit and secondary minimum to an occultation of the smaller component in an orbit with an inclination close to 90 degrees. The minima are of unequal depth, indicating unequal surface brightness of the components. Secondary minimum occurs very close to phase 0.5, suggesting a circular orbit, which is expected from tidal evolution of highly distorted stars. The depths in intensity of primary and secondary minima are 0.36, 0.78, 0.36, 0.81, and 0.38, 0.79 in the *UBV* bands, respectively.

4. ALL-SKY PHOTOMETRY

Transformations to the Johnson *UBV* system were determined by observing standard stars in E1 and E2 from the catalog of Menzies et al. (1989) during two photometric nights during the 1995 run. Table 1 shows the all-sky values obtained for the comparison and check stars, together with the RMS of the fit. Mean differential values of NP Pav in the maxima, in the sense NP Pav $-$GSC 9308:1513 are: $0^m.42$, $0^m.44$ and $0^m.39$ for U, B, and V, respectively.

To reduce these observations we used the package for reduction, transformation to standard system, archiving and retrieval of photometric observations, developed by Harmanec, Horn, & Juza (1994). The main program of the package is very flexible and quick. It reduces all observing data for a given night or a whole observing season, employing all suitable comparison and check stars as standard stars for the calculation of the coefficients.

5. PHOTOMETRIC SOLUTIONS

5.1. *Weighting Scheme, Control Integers and Assumptions*

Index 1 here refers to the component that is eclipsed at primary minimum. A detailed explanation of the control integers, modes of operation, subroutines, and all the mathematics involved in the WD program can be found in Wilson (1992; 1993).

Magnitudes were converted into intensities. Curve-dependent (SIGMA) weights were calculated measuring the standard deviations in sections of each light curve judged to be typical (phases 0.20–0.30 and 0.70–0.80). The resulting mean standard deviations from a linear least squares fit in the above intervals are depicted in Table 2. Level dependent (NOISE) weights were obtained by comparing the above standard deviations with those in the minima (least-squares fit between phases 0.98–0.02 and 0.48–0.52) and are also depicted in Table 2. Intrinsic weights equal to the number of individual points have been assigned to the normal points when these were used in the calculations.

A fine surface grid (N1, N2, NL1, NL2) and symmetrical partial derivatives for each of the adjustable parameters (ISYM) were adopted during all the calculations. Multiple reflexions (MREF, NREF) were not allowed for; L_2, the relative luminosity of the eclipsing component at primary minimum, has been kept coupled (IPB) to T_2 through the Planck function; at the final stages of the solution, it was liberated. The atmospheric option (IFAT1, IFAT2) was used with component 1 equal to one, and in the final stages of the solution was set equal to zero. These values are also depicted in Table 2. Increments in the adjustable parameters (independent variables)

TABLE 1

ALL-SKY VALUES FOR THE COMPARISON AND CHECK STARS OF NP PAV

	Comparison=GSC 9308:1513	Check #1=GSC 9321:1105	Check #2=GSC 9308:1782	RMS
V	10.559 ± 0.002	6.867 ± 0.004	8.102 ± 0.003	0.003
$U-B$	0.149 ± 0.002	-0.159 ± 0.001	0.146 ± 0.003	0.004
$B-V$	0.145 ± 0.001	-0.052 ± 0.002	0.523 ± 0.002	0.002
$V-R_{c}$	-0.065 ± 0.002	0.035 ± 0.001	-0.296 ± 0.002	0.001
$R_{c}-I_{c}$	-0.067 ± 0.005	0.043 ± 0.003	-0.274 ± 0.003	0.003

TABLE 2

CURVE- AND LEVEL-DEPENDENT WEIGHTS, CONTROL INTEGERS ADOPTED AND LIMB-DARKENING COEFFICIENTS ASSUMED

Wavelenght[Å]		SIGMA		NOISE
3500		0.0112		1
4500		0.0086		1
5550		0.0086		1
MREF, NREF	1		1	
ISYM, IPB	1		0 or 1	
IFAT1, IFAT2	1 or 0		0	
N1, N2, NL1, NL2	30	24	19	17
	x_1	y_1	x_2	y_2
bol	0.671	0.195	0.644	0.163
U	0.723	0.262	0.863	-0.205
B	0.820	0.335	0.854	-0.018
V	0.711	0.291	0.800	0.116

have been kept fixed at their default values. The MMS method of multiple subsets (Wilson & Biermann 1976; Wilson 1988) was used during all the calculations, making subsets of one parameter each.

Based on the $(B-V)$ color of the light curves, the temperatures of the components were assumed to be 8000 and 5200°K. The color of the bright component is $(B-V)_{II} = 0.183$, and supposing zero reddening ($\beta = -35°.49$), the work of Popper (1980) gives A6, implying $\log T_{eff} = 3.9$. For the secondary component $(B-V)_{I} = 0.233$, but since this value is contaminated, we assume a type of approximately K0. Starting parameters for the gravity'darkening exponents (g_1, g_2) and bolometric albedos (A_1, A_2) were taken as the appropriate values for the radiative and convective atmospheres for components 1 and 2, respectively. To describe the center-to-limb darkening of the stellar surfaces, the non-linear logarithmic law was assumed (LD=2). Bolometric and wavelenght-dependent limb-darkening coefficients (x_{1b}, y_{1b}, x_{2b},

y_{2b}, $x_{1\lambda}$, $y_{1\lambda}$, $x_{2\lambda}$, $y_{2\lambda}$) were taken from Van Hamme (1993) for log $g = 4.0$ and solar abundances. These values are given in the lower part of Table 2. No third light was allowed for, and a circular orbit and synchronous rotation were assumed.

5.2. *Normal Points, (q, i versus SS)-Grid and Solutions Based on Normal Points*

We first calculated normal points. 140 normal points were derived by averaging the individual observations at 0.005 phase intervals between phases 0.90–0.10 and 0.40–0.60, and at 0.010 phase intervals in the remaining light curve. With these normal points, we constructed the archive DC.IN (the archive for the DC program) together with the values and the assumptions of § 5.1. We built a grid to test the parametric n-dimensional space and identified the principal minimum. We selected the mass ratio q and the inclination i as the most sensible parameters, and the check was the *SS*, that is, the sum of squares of weighted residuals. For q we chose values of: 0.2, 0.3, 0.4, 0.5, 0.6, 0,7, 0.8, 0.9, 1.0, 1.1, 1.2, 1.3, 1.5, 2.0, 3.0 and 5.0; for i we chose values of: 70, 75, 80, 85, 87.5, and 90.

For this set of 16×6 distinct values, we constructed a solution and calculated the corresponding *SS*. The number of iterations varied from 60 to 180, so as to obtain an error between 0.1 and 0.3. We used Mode 2 and set the values of the potentials to be inside the respective Roche lobes of the components in the first iteration. The adjustable parameters were the phase shift $\phi = 0$, the mean surface temperature of secondary component, T_2, the modified normalized surface potentials of the components Ω_1, Ω_2, and the monocromatic relative luminosity of the primary component $L_1 = 12,000$. The result is depicted in Figure 1. The smallest value of *SS* was 0.0523, corresponding to $q = 0.5$ and $i = 87.5$ degrees.

With these parameters, we included q and i as adjustable parameters in the solution. This solution
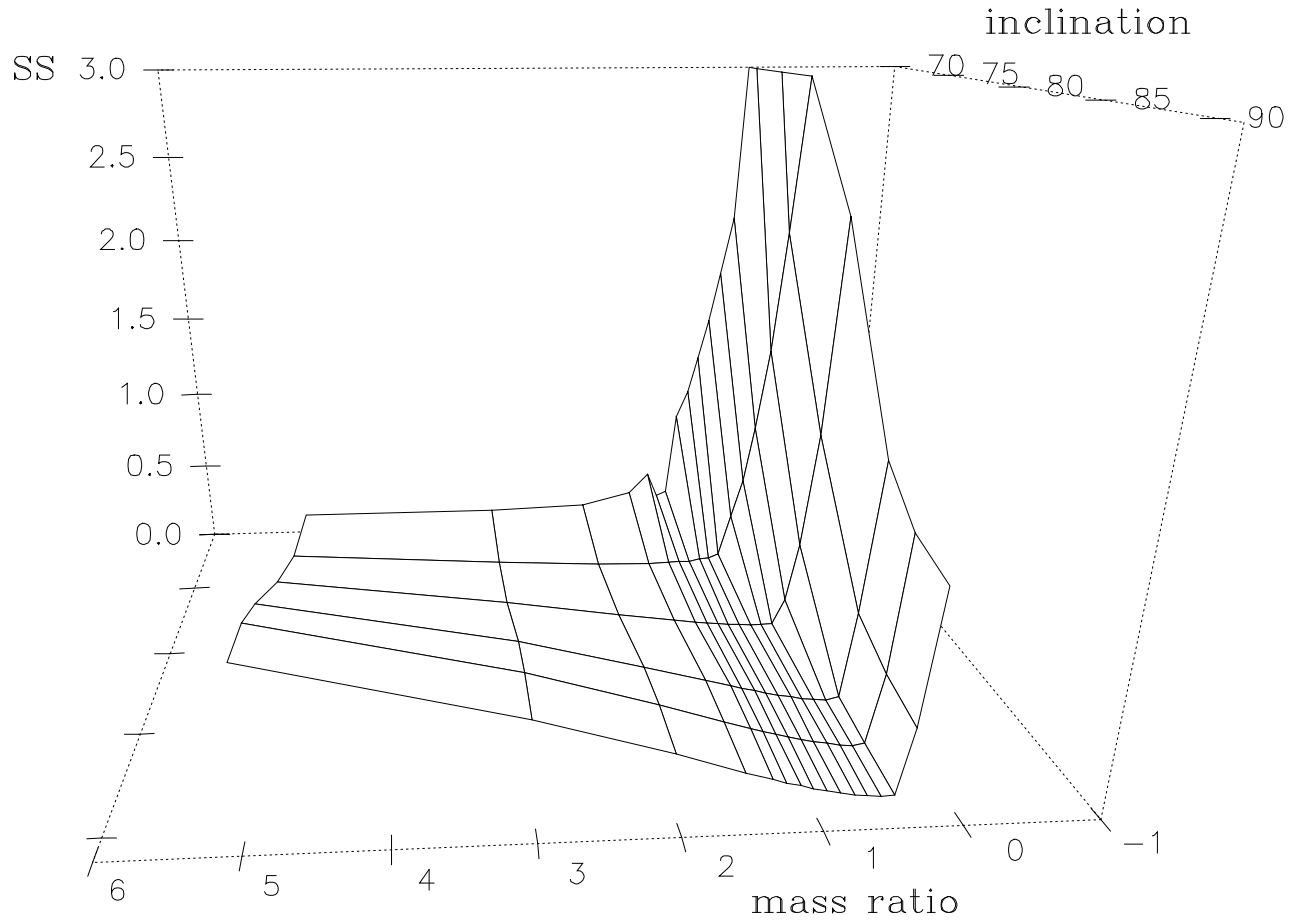
Fig. 1. Grid *(q, i)* versus *SS*.

is labeled *I* in Table 3.

The adjusted parameters are those quantities accompanied by the (internal) probable errors, except for the radii, which are functionally determined by q and Ω. We also computed a solution considering the set of astrophysical parameters together with the main parameters. We took as adjustable parameters g_1, the gravity darkening exponent of component 1, A_2, bolometric albedo for star 2, and $x_{1\lambda}$, the wavelenght-dependent limb-darkening coefficient for star 1. These are the coefficients that are recoverable from the observations and the physical model embedded in the WD program (see Cerruti 1996), as expected from the low light contribution of the secondary. This is the solution labeled *II* in Table 3.

5.3. *Individual Observations and Solutions*

Next, we began to construct solutions with the individual observations. Solution *III* of Table 3 has the following adjustable parameters: ϕ, i, g_1, T_2,

A_2, Ω_1, Ω_2, q, $L_{1\lambda}$, and $x_{1\lambda}$. We computed this solution first with the principal parameters and then we added the three astrophysical parameters. As in the previous section, the model with the astrophysical parameters represents well the observations, except for the filter U, where in the model the depth of the secondary minimum is approximately 0.03 magnitudes higher than in the observations, and the depth of the primary minimum is approximately 0.01 magnitudes higher than in the observations. This is common in Algol systems, since the temperatures of the components are very different, and radiation theory is severely tested and often may prove inadequate (see for example U Sge and RY Per [Van Hamme & Wilson 1986]). Also, the astrophysical parameters g_1 and the $x_{1\lambda}$ have values greater than 1. We also ran the program in mode 5, where the secondary is compelled to fill out its Roche lobe. The result was the same as above, and the *SS* is also practically the same. This is solution *IV* of Table 3. We also made two solutions altering the value of IFAT. In
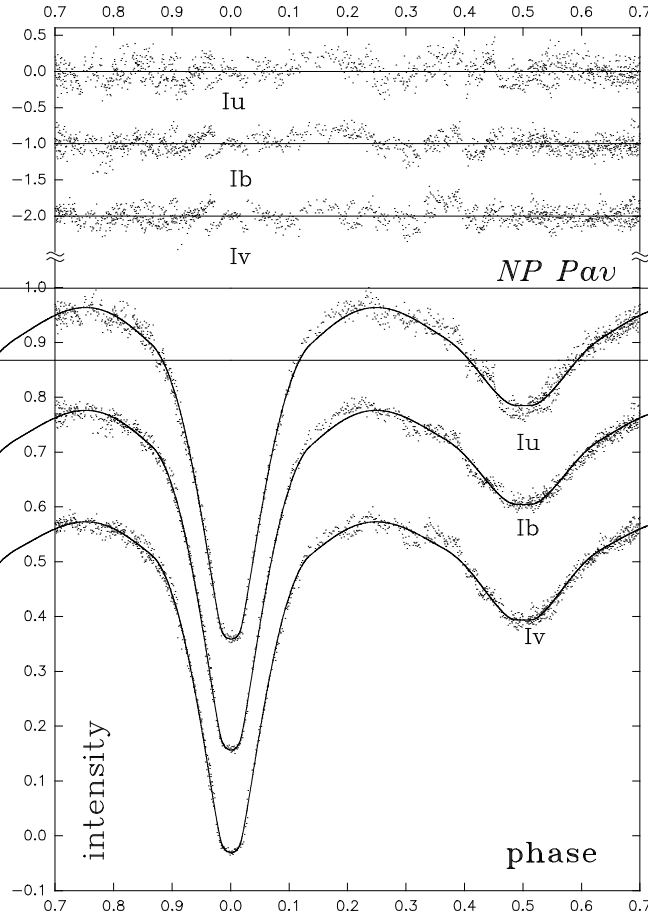
Fig. 2. *UBV* differential observations of NP Pav against our fitted model curves for our adopted solution *VI*. The light curves are vertically shifted by 0.2. Residuals are shown in the upper part of the figure.

one solution we used IFAT1=IFAT2=1, in the other IFAT1=IFAT2=0; the stellar atmosphere radiation theory does not change anything, while the black-body radiation theory adjusts the primary minimum. This is solution *V* of Table 3, which also adjusts the astrophysical parameters g_1 and $x_{1\lambda}$ to values less than 1. The other thing that can be done is to set the integer IPB=1, that is, to remove the constraint on L_2, the relative secondary luminosity at each wavelength, that is computed from the temperatures and other parameters. The change of IPB made L_2 an adjustable parameter. A solution with this L_2 is labeled *VI* in Table 3, and this will be our adopted solution. This solution made an improvement in the secondary U minimum; the difference between the model and the observations is 0.01 mag. There is also a difference of 0.005 mag in the phase interval 0.13 to 0.20 in the three filters, the observations having larger intensities than the model. This minor effect can perhaps be solved by a spot on one com-

ponent, and this will be calculated when we have a new light curve at our disposal. The light curve is shown in Figure 2.

6. DISCUSSION AND CONCLUSIONS

We have used solution *VI* to estimate the absolute dimensions. Masses can be calculated with the assumption that the more massive star is a normal main-sequence star that follows the mass-luminosity relation. The luminosity can be replaced by the absolute radius and temperature using the radiation law; the absolute radius can be replaced by the mass ratio, period, and radius by means of the third law of Kepler. Taking from Popper (1980) $T_{\rm eff} = 5780$ and $M_{\rm bol} = 4.64$, and using as the intercept and slope of the mass-luminosity relation 4.6 and 10, one obtains the main component. With the mass ratio one obtains the $\mathcal{M}_2$. These are shown in Table 4.

We estimate that the typical external error for the radii is 1%. The estimate for the error in the

TABLE 3

SOME OF THE SOLUTIONS[a]

	I	II	III	IV	V	VI
ϕ	0.0007±0.0001	0.0007±0.0001	0.0006±0.0001	0.0006±0.0001	0.0006±0.0001	0.0006±0.0001
i [deg]	87.851 ±0.557	86.093 ±0.488	87.348 ±0.227	79.829 ±0.163	89.191 ±0.501	89.100 ±0.439
g_1	1.000	0.766 ±0.056	0.857 ±0.030	0.901 ±0.028	0.984 ±0.025	0.647 ±0.028
g_2	0.320	0.320	0.320	0.320	0.320	0.320
$T_1[^oK]$	8000	8000	8000	8000	8000	8000
$T_2[^oK]$	5030 ± 23	4972 ± 40	4911 ± 20	4732 ± 20	4901 ± 16	6670 ±135
A_1	1.000	1.000	1.000	1.000	1.000	1.000
A_2	0.500	1.050 ±0.048	1.016 ±0.024	1.094 ±0.024	0.630 ±0.020	0.433 ±0.019
Ω_1	3.0402±0.0110	2.8521±0.0123	2.9056±0.0064	3.0698±0.0095	3.0386±0.0091	3.0268±0.0057
Ω_2	2.8631±0.0229	2.7325±0.0161	2.8028±0.0072	2.8048±0.0095	2.8810±0.0098	2.8811±0.0094
$q=\mathcal{M}_2/\mathcal{M}_1$	0.4777±0.0067	0.3972±0.0053	0.4163±0.0025	0.4634±0.0039	0.4769±0.0038	0.4889±0.0038
$L_1/(L_1+L_2)\_3500$	0.9709±0.0000	0.9797±0.0000	0.9813±0.0000	0.9814±0.0000	0.9783±0.0000	0.9411±0.0018
$L_1/(L_1+L_2)\_4500$	0.9552±0.0001	0.9669±0.0001	0.9691±0.0001	0.9671±0.0001	0.9569±0.0001	0.9403±0.0015
$L_1/(L_1+L_2)\_5550$	0.9260±0.0002	0.9443±0.0002	0.9492±0.0001	0.9415±0.0002	0.9334±0.0001	0.9215±0.0013
$L_2/(L_1+L_2)\_3500$						0.0589±0.0018
$L_2/(L_1+L_2)\_4500$						0.0597±0.0015
$L_2/(L_1+L_2)\_5550$						0.0785±0.0013
x_{1_3500}	0.723	1.236 ±0.035	1.174 ±0.017	1.398 ±0.024	0.782 ±0.025	0.742 ±0.023
x_{1_4500}	0.820	1.344 ±0.033	1.298 ±0.016	1.553 ±0.025	0.872 ±0.024	0.805 ±0.022
x_{1_5550}	0.711	1.286 ±0.033	1.246 ±0.016	1.495 ±0.025	0.815 ±0.025	0.741 ±0.024
x_{2_3500}	0.770	0.770	0.770	0.770	0.770	0.770
x_{2_4500}	0.817	0.817	0.817	0.817	0.817	0.817
x_{2_5550}	0.801	0.801	0.801	0.801	0.801	0.801
% filling star 1	93	94	93	91	93	94
% filling star 2	99	98	99		98	99
r_1 pole	0.3854±0.0009	0.4026±0.0016	0.4044±0.0009	0.3793±0.0010	0.3856±0.0006	0.3889±0.0005
r_1 point	0.4454±0.0014	0.4675±0.0034	0.4654±0.0017	0.4313±0.0015	0.4456±0.0011	0.4549±0.0012
r_1 side	0.4037±0.0010	0.4235±0.0020	0.4253±0.0011	0.3962±0.0011	0.4039±0.0008	0.4081±0.0006
r_1 back	0.4217±0.0010	0.4415±0.0023	0.4420±0.0012	0.4121±0.0012	0.4218±0.0008	0.4275±0.0007
r_2 pole	0.2910±0.0062	0.2710±0.0048	0.2695±0.0025	0.2938±0.0007	0.2876±0.0028	0.2935±0.0027
r_2 point	0.3756±0.0324	0.3360±0.0171	0.3443±0.0115	0.4217±0.0028	0.3621±0.0118	0.3812±0.0159
r_2 side	0.3029±0.0073	0.2811±0.0057	0.2799±0.0030	0.3066±0.0007	0.2989±0.0033	0.3056±0.0033
r_2 back	0.3323±0.0114	0.3072±0.0087	0.3084±0.0047	0.3391±0.0007	0.3266±0.0051	0.3354±0.0052
SS final	0.0517312	0.0417601	0.0977603	0.1002494	0.0915132	0.0844760

[a]See text for explanations.

temperatures is 4%, corresponding to one spectral subclass. The typical external error should be about 3% for q, and negligible for P. Knowing the masses, the rest of the absolute elements can be obtained, and they are shown in Table 4. In the lower part of this table, we also list radii, masses, and luminosities corresponding to normal MS stars (not ZAMS values) of the same effective temperature (Harmanec 1988). The absolute dimensions of the primary component is similar to that of a normal MS star. The secondary seems to be oversized for its mass, and sub-luminous.

We have plotted the limiting error box of the main characteristics of the components of NP Pav in the HR, MR, and ML diagrams. In the HR dia-

gram, the primary resembles a normal MS star (close to the ZAMS) that is entering the region of normal MS stars, while the secondary is out of the MS region but not on the red subgiant region. It is below the MS, on the region of the secondaries of WUMa stars. On the MR plane, the primary occupies the same region as in the previous diagram, but the secondary is on the red subgiant region. In the ML diagram, both components are located as in the HR diagram. However, the errors are larger, in particular for the companion.

NP Pav is therefore a short-period system. According to the light curves it can be classified between an Algol-like and a β Lyrae-like system. The components and the orbit appear, in general, to be
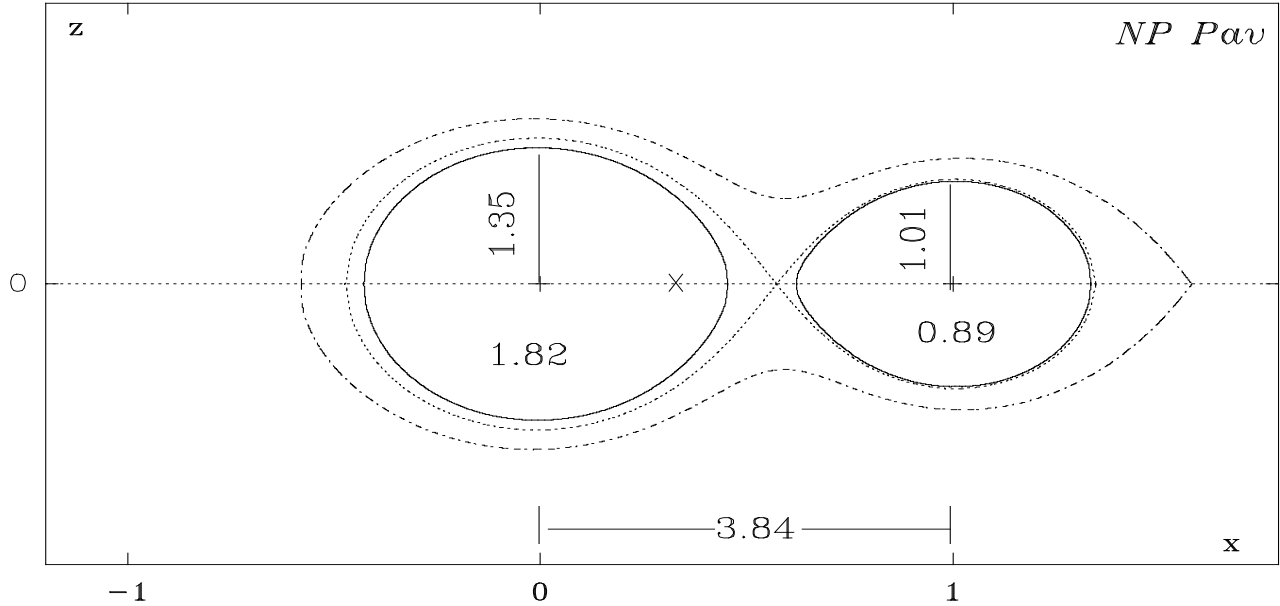
Fig. 3. Configuration of NP Pav at phase 0.25 for solution *VI*. Dashed lines indicate inner and outer Roche equipotential surfaces. The cross corresponds to the center of gravity of the system. Masses, radii, and separations of the components are given in solar units.

TABLE 4

ABSOLUTE DIMENSIONS AND RELATED
QUANTITIES FOR NP PAV

$\mathcal{M}_1/M_\odot$	1.82 ± 0.20
$\mathcal{M}_2/M_\odot$	0.89 ± 0.10
$\mathcal{R}_1/R_\odot$	1.35 ± 0.19
$\mathcal{R}_2/R_\odot$	1.01 ± 0.14
$\mathcal{L}_1/L_\odot$	9.03 ± 0.90
$\mathcal{L}_2/L_\odot$	1.81 ± 0.18
$\mathcal{A}[R_\odot]$	3.84 ± 0.54
$\mathcal{M}_1/M_{\odot,\mathrm{MS}}$	1.81
$\mathcal{M}_2/M_{\odot,\mathrm{MS}}$	1.40
$\mathcal{R}_1/R_{\odot,\mathrm{MS}}$	1.81
$\mathcal{R}_2/R_{\odot,\mathrm{MS}}$	1.48
$\mathcal{L}_1/L_{\odot,\mathrm{MS}}$	11.42
$\mathcal{L}_2/L_{\odot,\mathrm{MS}}$	3.70

stable but the possibility of a spot should be kept in mind. The temperature difference between the components is $\Delta = 1330°$K. The primary resembles an MS A6V star, and it is detached from its lobe (94%), while the secondary nearly fills its lobe (99%) and its spectral class is F2. No attempt was made to compare NP Pav with objects of similar characteristics, nor to discuss their evolutionary scenario based on the absolute elements, because we consider our results as very preliminary ones, since the method employed for the determinations of absolute dimensions is rather uncertain. The configuration of the system is depicted in Figure 3. Spectrographic data will substantially improve the absolute elements given here.

REFERENCES

Cerruti, M. A. 1996, Acta Astron., 46, 429
_____. 2000, IAU IBVS, 4956
Harmanec, P. 1988, Bull. Astron. Inst. Czechosl., 39, 329
Harmanec, P., Horn, J., & Juza, K. 1994, A&AS, 104, 121
Hoffmeister, C. 1949, Erg. Astronom. Nachr., 12, No. 1
_____. 1957, Mitt. Veränd. Sterne, 1, 245
Kang, Y. W., & Wilson, R. E. 1989, AJ, 97, 848
Kukarkin, B. V., Kholopov, P. N., Kukarkina, N. P., & Perova, N. P. 1972, IAU IBVS, 717
Menzies, J. W., Cousins, A. W. J., Banfield, R. M., & Laing J. D. 1989, South African Astron. Obs. Circ., 13, 1

Popper, D. M. 1980, ARA&A, 18, 115
Schmidt, E. G. 1992, IAU IBVS, 3733
Shaw, S., & Sievers J. 1970, Bamberg Veröff., VIII, 90
Van Hamme, W. 1993, AJ, 106, 2096
Van Hamme, W., & Wilson, R. E. 1986, AJ, 92, 1168
Wilson, R. E. 1979, ApJ, 234, 1054
_____. 1988, in Critical Observations Versus Physical Models for Close Binary Stars, ed. K.-C. Leung (Gordon and Beach Science Publishers), 193

_____. 1990, ApJ, 356, 613
_____. 1992, Documentation of Eclipsing Binary Computer Model, privately circulated monograph
_____. 1993, in ASP Conf. Ser. Vol. 38, New Frontiers in Binary Star Research, eds. K.-C. Leung & I. S. Nha (San Francisco: ASP), 91
Wilson, R. E., & Biermann, P. 1976, A&A, 48, 349
Wilson, R. E., & Devinney. E. J. 1971, ApJ, 166, 605

Miguel Angel Cerruti: Instituto de Astronomía y Física del Espacio, CC 67, Suc. 28, C1428 Buenos Aires, Argentina (miguelan@iafe.uba.ar).